Absorption of Beta Particles in Al and Cu: Determination of Mass Attenuation Coefficients

Ziyao Xiong

***Abstract*—This experiment conducted an in-depth examination of beta particle absorption in Aluminum and Copper, employing a ^{90}Sr source. Count rates across varying thicknesses of Al and Cu sheets were measured. Minimum chi-square fitting identified the ranges of beta particle penetration and the maximum energy of particles. Mass attenuation coefficients for Al and Cu were calculated as 6.69±0.26 g/cm^2 and 10.24±0.33 g/cm^2, respectively.**

I. Introduction

BETA Beta particles are high-energy electrons or positrons emitted from nuclear decay, exhibit distinctive interactions with matter, leading to their gradual attenuation over distance [1]. Aluminum (Al) and copper (Cu) are frequently used in applications requiring radiation protection due to their capacity to attenuate beta particles [2]. This lab report focuses on determining the mass attenuation coefficient of beta particles as they pass through sheets of Al and Cu, aiming to provide a quantitative measure of how these materials can reduce the intensity of beta radiation.

II. Theory

As depicted in Fig. 1, our experiment employed a Strontium-90 radioactive source, leading to β-particle emissions with three distinct E_{max} values: $^{90}Sr \rightarrow {}^{90}Y$ transitions produce β-particles of 0.54 MeV (E_{max1}), and $^{90}Y \rightarrow {}^{90}Zr$ transitions result in β-particles of 2.27 MeV (E_{max2}) [3]. A minor fraction of the decays also emit β-particles with 0.51 MeV (E_{max3}), subsequently generating γ radiation contributing to background radiation [3]. Owing to its rarity (0.02%), these occurrences were excluded from our analysis. Given the minimal attenuation of γ radiation by Al and Cu [4], its removal from our measurements was imperative, focusing our study solely on β-particle attenuation.

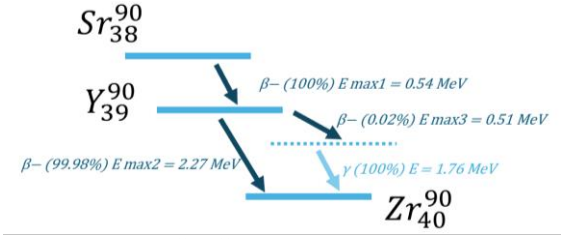

Fig.1. Decay process of ^{90}Sr. ^{90}Sr proceeds through β^- emission, leading to the creation of Yttrium-90 (^{90}Y), which itself is a beta-emitter, eventually stabilizing as Zirconium-90 (^{90}Zr).

β-rays are absorbed in matter upon losing their energy. The range, defined as the mass thickness of the material that β-particles can traverse before being absorbed through atomic interactions [5].

E_{max} of a beta emission directly influences the range of the particles. Higher energy β-particles exhibit longer ranges due to greater kinetic energy loss capacity. The relationship between E_{max} and range R can be described by:

$$R(g/cm^2) = 0.11\left(\sqrt{1 + 22.4E_{max}^2} - 1\right). \quad (1)$$

As β-particles traverse a material, their intensity I decreases with thickness of material x exponentially, described by Beer Lambert Law [6]:

$$I = I_0 e^{-\mu x}, \quad (2)$$

where I_0 is initial intensity and μ is the linear attenuation coefficient of the material, which represents the probability per unit path length of a β-particle being absorbed by the material. It is dependent on the energy of the β-particles and the properties of the material (such as atomic number Z and density ρ). The mass attenuation coefficient (μ/ρ) normalizes μ by the material's density, providing a measure of attenuation that is independent of the material's physical state. It can be calculated by:

$$\mu/\rho = \frac{7.7Z^{0.31}}{E_{max}^{1.14}}. \quad (3)$$

III. Mathod

As shown in Fig. 2, Al/Cu sheets were positioned horizontally atop the silicon detector, functioning as a 300 μm thick insulator with a 50 V applied voltage [3]. To optimize count capture and minimize solid angle effects, the separation between the source and detector was established at 5 cm, based on preliminary findings. Subsequent layers of Al/Cu sheets were added onto the detector, with the cumulative thickness gauged at three points using a micrometer at each stage. The variability in thickness can be attributed to the sheets' propensity for bending or possessing uneven surfaces. Average thicknesses and associated uncertainties were recorded, where uncertainties were derived from the standard deviation of repeated measurements.

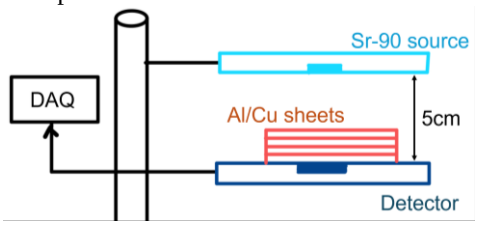

Fig.2. Apparatus set-up. The silicon detector is connected to the computer with Data Acquisition Program (DAQ) that can count the number of decays in a given time frame.

Count rates were calculated by dividing the total detected counts by the recording time. Measurements were conducted over 10 cycles, each lasting 10 seconds, to average out random uncertainties and identify outliers effectively. The chosen duration, significantly exceeding the detector's ~2μs dead time, ensures data quality and accommodates accurate count measurements at increased thicknesses.

The uncertainty in the count rate, stemming from radioactive decay's statistical nature, aligns with a Poisson distribution, where the standard deviation (σ) of decay events (n) equals $\sqrt{n}$. For analysis on a natural log scale, error propagation formula is used to find the uncertainty in $ln\ n$:

$$\sigma(\ln n) = \left|\frac{d(\ln n)}{dn}\right| \sigma n = \frac{\sqrt{n}}{n}. \quad (4)$$

IV. Results, Analysis, and Discussions

A. Elimination of background radiation

Per Equation (2), the count number versus thickness exhibits exponential decay; thus, the natural logarithm of count numbers is taken to demonstrate a linear relationship, as depicted in Fig. 3. The curve can be categorized into three regions: initially, both low-energy β-particles from ^{90}Sr and high-energy β-particles from ^{90}Y penetrate the Al sheets. In the intermediate region, only high-energy β-particles can traverse the thicker Al. At maximum thickness, all β-particles are absorbed, leaving only background γ radiation.

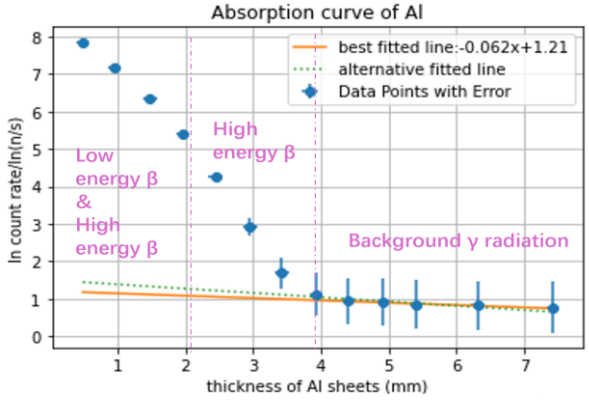

Fig. 3. Aluminum absorption curve, illustrating two potential fittings for background radiation. The solid line represents the selected fitting (initiated from 8th point), while the dashed line indicates the non-selected alternative (initiated from 7th point). The fitted line is y=-0.062x+1.21.

To mitigate background radiation effects, identifying when all β-particles are absorbed is essential, leaving only gamma radiation, which manifests as a linear trend in the data. Linear fits initiated from the 7th and 8th data points—identified as potential transition points—yielded chi-square values of 0.16 and 0.013, respectively. The lower chi-square for the 8th data point indicates it as the transition to exclusively gamma radiation, thereby selecting it for subsequent analysis.

B. Two-line fitting

Subtracting the fitted line for gamma radiation from the dataset isolates the beta particle absorption spectrum, illustrated in Fig. 4. To distinguish between high and low energy beta particles, straight line fittings were applied to segments before and after each potential data cut. The chi-square values for the fit lines pre- and post-cut were summed, selecting the cut with the smallest chi-square total.

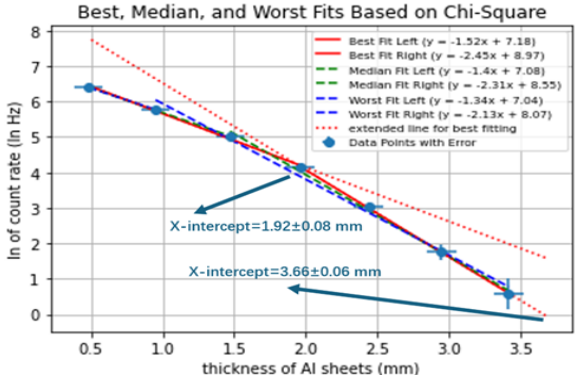

Fig.4. Aluminum absorption curve after eliminating the background radiation. The best, median, worst two-line fittings were showed, with ascending chi-square values. The best fitting lines were extrapolated to determine their x-intercepts.

The x-intercept of the two-line intersection indicates complete absorption of low-energy particles, while the right-side extended line's x-intercept denotes full absorption of high-energy particles, found at 1.92±0.08 mm and 3.66±0.06 mm, respectively. By multiplying the thickness by the material's density—2.7 g/cm^3 for Al and 8.96 g/cm^3 for Cu—the ranges for low and high energy beta particles were calculated as 0.52±0.05 g/cm^2 and 0.99±0.04 g/cm^2, respectively. Maximum energies, derived from Equation (1), were 1.19±0.19 MeV for low and 2.19±0.13 MeV for high energy particles. Compared to theoretical E_{max1} (0.54 MeV) and E_{max2} (2.27 MeV), E_{max2}'s experimental value aligns well within uncertainty, whereas E_{max1} deviates by 120%, suggesting incomplete separation of particle energies. This implies that the optimal separation point precedes the identified one by a significant amount, indicating a predominance of high-energy particles from ^{90}Y in the source. Consequently, we choose to assume there only exist high-energy particles with E_{max2} in the absorption curve.

C. One line fitting

As shown in Fig.5., a single straight line fitting was applied to the absorption curves of Al and Cu, identifying the maximum thickness high-energy particles can penetrate: 3.87±0.05 mm for Al and 1.09±0.06 mm for Cu. Calculated E_{max} values were 2.21±0.13 MeV for Al and 2.17±0.16 MeV for Cu, aligning well with the theoretical 2.27 MeV, validating our single-energy model. With atomic numbers 13 (Al) and 29 (Cu), the mass attenuation coefficients were determined to be 6.69±0.26 g/cm^2 for Al and 10.24±0.33 g/cm^2 for Cu, consistent with expectations given Cu's higher atomic mass and its resultant increased probability for scattering and Bremsstrahlung, thus more effectively reducing beta radiation intensity.

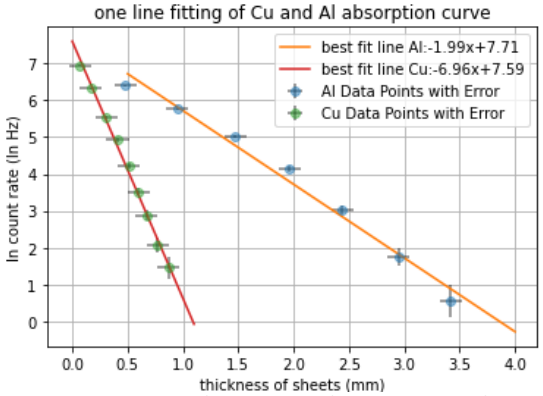

Fig.5. Absorption curve of Al and Cu after elimination of background radiation. Best fitted lines were determined by the least chi-square method.

V. Conclusion

In our investigation, we analyzed the maximum energy of beta particles by applying two-line fittings to the absorption curves, aiming to distinguish between the maximum energies of particles emitted by ^{90}Sr and ^{90}Y. The analysis revealed significant discrepancies for low-energy particle emissions, leading to the inference that the majority of decay products are high-energy particles originating from ^{90}Y. Subsequently, a single-line fit to the Al and Cu absorption curves, yielded maximum energies in line with the theoretical expectations for ^{90}Y decays. Furthermore, the calculated mass attenuation coefficients, with copper exceeding aluminum, matched our predictions. However, due to resource constraints, it was not feasible to acquire theoretical mass attenuation coefficient values for the specific energies measured, preventing a direct accuracy evaluation. Thus, our results are deemed consistent with theoretical anticipations, albeit without direct verification of the mass attenuation coefficients' precision.

REFERENCES

[1] J. Konya and N. M. Nagy, Nuclear and Radiochemistry. Elsevier, 2012, pp. 74–75. ISBN: 978-0-12-391487-3.

[2] J. Konya and N. M. Nagy, Nuclear and Radiochemistry. Elsevier, 2012, pp. 74–75. ISBN: 978-0-12-391487-3.

[3] Imperial College London Physics Department, "The Second Year Laboratory: Radioactivity experiment," London, 2024.

[4] Y. Wang, Ed., CRC Handbook of Radioactive Nuclides, Chemical Rubber Company, Ohio, 1969.

[5] C. S. Mahajan, "Mass attenuation coefficients of beta particles in elements," Science Research Reporter, vol. 2, no. 2, pp. 135-141, 2012.

[6] P. Bouguer, Essai d'optique sur la gradation de la lumière, Claude Jombert, Paris, France, 1729, pp. 16–22.